ELSEVIER

International Journal of Heat and Fluid Flow 22 (2001) 643–649

International Journal of HEAT AND FLUID FLOW

www.elsevier.com/locate/ijhff

Periodic oscillations in a horizontal single boiling channel with thermal wall capacity

P.R. Mawasha [a,*], R.J. Gross [b]

[a] *Wright State University, Dayton, OH 45436-0001, USA*
[b] *College of Engineering, The University of Akron, Akron, OH 44325-3901, USA*

Received 8 February 2001; accepted 17 May 2001

Abstract

The dynamic behavior of a horizontal boiling channel with a surge tank is investigated through nonlinear analysis. The model involves a surge tank that is subject to inlet mass flow rate and a constitutive model containing a cubic nonlinearity is used to describe the outlet pressure-flow rate relation of the downstream boiling regime. The model also includes boiling heat transfer process and incorporates the effect of the wall thermal capacity which allows the temperature and heat transfer coefficient of the heater wall to vary with time. Within certain operating regimes, the model exhibits self-excited periodic oscillations, which can be identified with pressure-drop oscillations. In this study, these oscillations are described as relaxation oscillation and the qualitative features of the response can be understood in terms of the underlying model. Finally, the present model is compared with the experimental data available in literature to investigate that transient effects of temperature heater walls, pressure, and mass flow rate.

Keywords: Boiling instabilities; Pressure-drop oscillation; Thermal wall capacity; Boiling heat transfer

1. Introduction

Single- and two-phase fluid flow dynamics in channels can be susceptible to linear and nonlinear effects. These nonlinearities could arise from interfacial forces between the flowing fluid and its walls, oscillations in fluid properties, thermal inertia or thermal wall capacity, growth of voids, etc. Fluid flow dynamics is prevalent in the application of heat exchanger design, nuclear reactors, cardiovascular flows, etc. Often, physical systems with single- and two-phase flows can undergo undesirable system operating scenarios leading to component failure.

The problem of understanding the dynamics and mechanisms of pressure-drop oscillations in a horizontal boiling channel with a surge tank has been studied extensively in boiling heat transfer. The modes of pressure-drop oscillations have previously been identified as pressure-drop oscillations in many studies (Yüncü, 1990; Yüncü et al., 1990; Stenning et al., 1967; Maulbetsch and Griffith, 1966). Pre-drop oscillations in a vertical boiling channel have been investigated (Padki et al., 1991, 1992; Kakaç et al., 1990; Gürgenci et al., 1976, 1983). The understanding of the dynamic, periodic, pressure-drop oscillations and other instabilities in channels owes its relevance to the design of nuclear reactors, heat exchangers, and power plant equipment, etc. Numerous studies of instabilities on heated channels are available in the literature (Kakaç, 1976; Kakaç and Veziroğlu, 1982).

To determine whether a system will oscillate, we studied the characteristics of the steady-state pressure difference versus mass flow rate curve for a boiling system. The steady-state curve or the nullcline of our system has the characteristics of a cubic function. From the cubic nullcline, it has been shown that for decreasing mass flow rate, boiling does not start to occur until the negative slope portion of the "steady-state pressure difference – mass flow rate" characteristic curve (Stenning et al., 1967). Also, other models In the present study, the "transient pressure difference – mass flow rate" curve or the phase plane of the system is being investigated to explain the limit cycle with features that give rise to sustained oscillations. These oscillations (pressure-drop oscillations) are characterized as relaxation oscillation and are similar to the behavior exhibited in the van der Pol oscillator (Strogatz, 1995; Van der Pol, 1927). Also, models with and without the effects of thermal wall capacity are compared.

The physical system utilized in the study is that of a surge tank partially filled with fluid, with isothermal expansion and compression of air above the fluid such that the pressure above the liquid varies with the liquid height. The surge tank is connected to a heated channel with a boiling fluid as depicted in Fig. 1.

* Corresponding author. Tel.: +1-937-775-5005; fax: +1-937-775-5009.

E-mail address: mawasha@cs.wright.edu (P.R. Mawasha).

0142-727X/01/$ - see front matter
PII: S0142-727X(01)00115-1

Notation

ρ	fluid density (kg/m^3)
μ	viscosity (N s/m^2)
μ_l	saturated liquid viscosity
$\dot{Q}$	convective heat transfer into the fluid
$\dot{Q}_H$	power input into the heater
A	pipe area
A_p	surface area of the heater
A_s	tank across sectional area
A_{si}	inlet flow area
C_f	coefficient of friction
c_H	specific heat capacity of the channel wall
C_s	surface condition of the fluid
D_e	effective diameter of the channel
F_F	frictional force
h	heat transfer coefficient of the fluid
H_s	liquid height
H_{si}	initial liquid height
H_{st}	surge tank height
h_v	latent heat of vaporization
k_w	thermal conductivity of the saturated fluid
L	pipe length
m	mass flow rate (kg/s)
m_H	mass of the channel wall
Nu	Nusselt number of the fluid
p_c	critical pressure of the fluid
p_g	gas pressure
p_{gi}	initial gas pressure
T_w	temperature of the channel wall
v	specific volume (m^3/kg)
W	mass flow rate
W	mass flow rate (kg/s)
x	average quality of the fluid

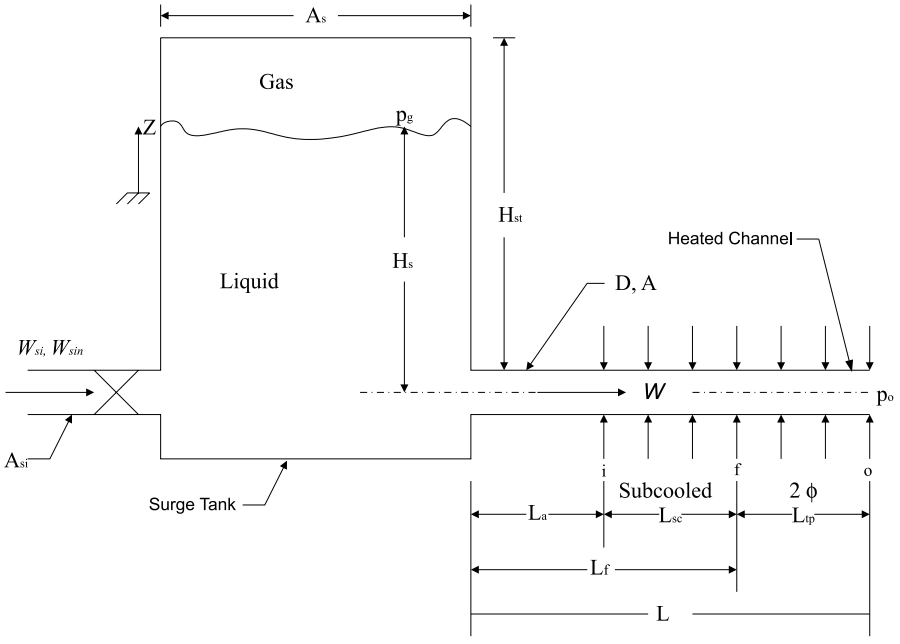

Fig. 1. Horizontal single boiling channel with a surge tank consisting of inlet and outlet flow conditions.

The model studied here is obtained from the continuity equation of the surge tank, Euler's equation from the surge tank inlet to outlet, and the linear momentum equation for a control volume enclosing the fluid inside the heated channel. The model also includes boiling heat transfer process that incorporates the effect of the wall thermal capacity which allows the temperature of the heater wall to vary with time. The heat transfer coefficient of the underlying model is obtained from a two-phase flow correlation (Padki et al., 1991).

Unlike previous models, the present model only utilizes a surge tank and does not incorporate the supply tank observed in their experiments that the mass flow rate at the entrance of the surge tank does not oscillate beyond 5% (Gürgenci et al., 1976). As a result, in this model we assume that the mass flow rate at the entrance of the surge tank is constant. Also, the present model accounts for the effects of kinetic energy at the liquid surface inside the surge tank and at the exit of the surge tank. Previously, the two-phase pressure drop across the channel has been taken using the two-phase friction multiplier as a function of exit quality (Padki et al., 1991; Gürgenci et al., 1976). In the present study, the steady-state pressure drop versus mass flow rate experimental data is obtained from literature, and takes the form of a cubic function (Yüncü, 1990). The system, including the cubic function is similar in form to the van der Pol oscillator, a nonlinear electrical circuit which provides a canonical model for self-excited nonlinear oscillations (Van der Pol, 1927).

2. Modeling description

We consider a surge tank with a gas entrained above a constant density liquid. The constant fluid density assumption, together with constant inlet mass flow rate imply that the mass flow rate leaving the surge tank $W(t)$, and the tank liquid surface oscillate in phase with respect to time. At time $t = 0$, the inlet mass flow rate is reduced instantaneously from a constant value W_{si} to another constant value W_{sin}. Applying the continuity equation to the surge tank gives

$$\frac{dH_s}{dt} = \frac{W_{sin} - W}{\rho A_s}, \tag{1}$$

where W_{sin} is the constant inlet mass flow rate into the surge tank for time $t \geqslant 0$, ρ is the fluid density, A_s is the surge tank cross-sectional area, and H_s is the tank liquid level height above the pipe centerline.

For an inviscid flow, Euler's equation for constant fluid density for a streamline from the surge tank inlet to the liquid surface inside the surge tank gives

$$\frac{\partial V}{\partial t} + V\frac{\partial V}{\partial s} + \frac{1}{\rho}\frac{\partial p}{\partial s} + g\frac{\partial z}{\partial s} = 0, \tag{2}$$

where s is the path distance along a streamline from the liquid level surface (or $s = 0$). Multiplying Eq. (2) by ds and integrating from the surge tank inlet to the surge tank liquid level gives

$$\frac{p_g - p_{si}}{\rho} + \frac{V_g^2 - V_{sin}^2}{2} + gH_s + \int_{si}^{g} \frac{\partial V}{\partial t}\,ds = 0, \tag{3}$$

where p_{si} and p_g are the respective pressures at the surge tank inlet and the liquid level surface. V_{si} and V_g are the respective velocities at the surge tank inlet and the liquid level surface. The velocity of the liquid at the surge tank inlet can also be described as

$$V_{sin} = \frac{W_{sin}}{\rho A}. \tag{4}$$

Using

$$\frac{\partial V}{\partial t} \approx \frac{1}{2}\left(\frac{dV_g}{dt} + \frac{dV_{si}}{dt}\right), \quad V_g = \frac{dH_s}{dt}, \quad \frac{dV_g}{dt} = \frac{d^2H_s}{dt^2}$$

gives

$$p_{si} = \frac{\rho H_s}{2}\frac{d^2H_s}{dt^2} + \frac{\rho}{2}\left(-\frac{dH_s}{dt}\right)^2 + \rho g H_s + p_g - \frac{W_{sin}^2}{\rho A^2}. \tag{5}$$

We now apply Euler's equation (2) for constant fluid density for a streamline from the surge tank liquid surface to the outlet (channel inlet). In this case, the path distance along a streamline from the liquid level surface (or $s = 0$) to the outlet. Multiplying Eq. (2) by ds and integrating from the liquid surface to the surge tank outlet gives

$$\frac{p_{so} - p_g}{\rho} + \frac{V_{so}^2 - V_g^2}{2} - gH_s + \int_{g}^{so} \frac{\partial V}{\partial t}\,ds = 0.$$

Using

$$\frac{\partial V}{\partial t} \approx \frac{1}{2}\left(\frac{dV_g}{dt} + \frac{dV_{so}}{dt}\right), \quad V_g = -\frac{dH_s}{dt}, \quad \frac{dV_g}{dt} = \frac{d^2H_s}{dt^2}$$

gives

$$\frac{p_{so} - p_g}{\rho} + \frac{V_{so}^2 - V_g^2}{2} - gH_s + \frac{H_s}{2}\left(-\frac{d^2H_s}{dt^2} + \frac{1}{\rho A}\frac{dW}{dt}\right) = 0, \tag{6}$$

where p_{so} is the pressure and V_{so} is the velocity at the surge tank outlet. The velocity of the liquid at the surge tank outlet can also be described as

$$V_{so} = \frac{W}{\rho A}, \tag{7}$$

where W is the channel inlet mass flow rate. Substituting $V_g = -dH_s/dt$ and Eq. (7) into (6) yields

$$p_{so} - p_g + \frac{\rho}{2}\left[\frac{W^2}{\rho^2 A^2} - \left(-\frac{dH_s}{dt}\right)^2\right] - \rho g H_s + \frac{\rho H_s}{2}\left(-\frac{d^2H_s}{dt^2} + \frac{1}{\rho A}\frac{dW}{dt}\right) = 0. \tag{8}$$

Substituting the continuity equation (1) into Eq. (8) yields

$$\frac{\rho H_s}{2}\left(1 + \frac{A_s}{A}\right)\frac{d^2H_s}{dt^2} + \frac{\rho}{2}\left[1 - \frac{A_s^2}{A^2}\right]\left(\frac{dH_s}{dt}\right)^2 + \frac{A_s W_{sin}}{A^2}\frac{dH_s}{dt} + \rho g H_s + p_g - p_{so} - \frac{W_{sin}^2}{2\rho A^2} = 0. \tag{9}$$

The linear momentum equation for a control volume (denoted by the c.v. subscript) enclosing the liquid in the horizontal channel from the surge tank outlet to the channel outlet is

$$\Sigma F_i = p_{so}A - p_a A - \Delta p A = \frac{d(mV)_{c.v.}}{dt}, \tag{10}$$

where Δp accounts for the frictional pressure loss plus the momentum change across the channel, A is the area of the pipe, p_{so} and p_a are the respective pressures at the surge tank outlet and the pipe outlet. We note that

$$\frac{d(mV)_{c.v.}}{dt} = \frac{d}{dt}\int_{z=0}^{L} (\rho A\,dz)V = \frac{d}{dt}\int_{z=0}^{L} W\,dz. \tag{11}$$

Assuming W changes slowly with time t (as happens in pressure drop oscillations), we expect W to change slowly with z so we use the approximation

$$\frac{d(mV)_{c.v.}}{dt} \approx L\frac{dW}{dt}, \tag{12}$$

where W is the channel inlet mass flow rate. The frictional pressure loss and the momentum change across the channel Δp is a function of the surge tank outlet mass flow rate and is representative of the inlet valve, unheated fluid region, subcooled fluid region, partial boiling region, and the exit valve. The steady-state pressure difference – mass flow rate characteristic or a cubic nullcline for the heated channel is the mathematical description of the empirical correlation for constant heat input boiling pressure difference determined from

$$\Delta p = a + bW - cW^2 + eW^3, \tag{13}$$

where Δp is a function of the surge tank outlet mass flow rate and is representative of the inlet valve, unheated fluid region, subcooled fluid region, partial boiling region, and the exit valve. Constants a, b, c and e are obtained from experimental data and W is the channel inlet mass flow rate (Yüncü, 1990). Substituting Eqs. (12) and (13) into Eq. (10) results in

$$p_{so} = \frac{L}{A}\frac{dW}{dt} + p_a + (a + bW - cW^2 + eW^3). \tag{14}$$

Substituting the continuity equation (1) into Eq. (14) yields

$$p_{so} = \frac{L}{A}\left(-\rho A_s\frac{d^2H_s}{dt^2}\right) + p_a + a + b\left(W_{sin} - \rho A_s\frac{dH_s}{dt}\right) - c\left(W_{sin} - \rho A_s\frac{dH_s}{dt}\right)^2 + e\left(W_{sin} - \rho A_s\frac{dH_s}{dt}\right)^3. \tag{15}$$

Substituting Eq. (15) into Eq. (9) yields

$$\rho\left[\frac{A_s L}{A}+\frac{H_s}{2}\left(1+\frac{A_s}{A}\right)\right]\frac{d^2H_s}{dt^2}+\frac{\rho}{2}\left[1-\frac{A_s^2}{A^2}\right]\left(\frac{dH_s}{dt}\right)^2 + \frac{A_s W_{sin}}{A^2}\frac{dH_s}{dt}+\rho g H_s + p_g - p_a - a - b\left(W_{sin}-\rho A_s\frac{dH_s}{dt}\right) + c\left(W_{sin}-\rho A_s\frac{dH_s}{dt}\right)^2 - e\left(W_{sin}-\rho A_s\frac{dH_s}{dt}\right)^3 - \frac{W_{sin}^2}{2\rho A^2}=0. \quad (16)$$

Assuming an isothermal gas expansion above the liquid level height gives

$$p_g = p_{gi}\left(\frac{H_{st}-H_{si}}{H_{st}-H_s}\right), \quad (17)$$

where p_{gi} is the initial gas pressure. Substituting Eq. (17) into (16) yields

$$\rho\left[\frac{A_s L}{A}+\frac{H_s}{2}\left(1+\frac{A_s}{A}\right)\right]\frac{d^2H_s}{dt^2}+\frac{\rho}{2}\left[1-\frac{A_s^2}{A^2}\right]\left(\frac{dH_s}{dt}\right)^2 + \frac{A_s W_{sin}}{A^2}\frac{dH_s}{dt}+\rho g H_s + p_g\frac{H_{st}-H_{si}}{H_{st}-H_s} - p_a - a - b\left(W_{sin}-\rho A_s\frac{dH_s}{dt}\right) + c\left(W_{sin}-\rho A_s\frac{dH_s}{dt}\right)^2 - e\left(W_{sin}-\rho A_s\frac{dH_s}{dt}\right)^3 - \frac{W_{sin}^2}{2\rho A^2}=0. \quad (18)$$

The effect of the changing wall temperature is

$$m_H c_H\frac{dT_w}{dt} = \dot{Q}_H - \dot{Q}, \quad (19)$$

where m_H is the mass of the channel wall and heater, c_H is the specific heat capacity of the channel wall and heater, T_w is the channel wall and heater temperature, $\dot{Q}_H$ is the power input to the heater, and $\dot{Q}$ is the power input to the fluid. $\dot{Q}$ is obtained through the effect of convection and is given by

$$\dot{Q} = hA_p(T_w - T), \quad (20)$$

where h is the heat transfer coefficient of the fluid and A_p is the heat transfer surface area of the channel. The heat transfer coefficient h, can be written as

$$h = \frac{Nu}{D}k_w, \quad (21)$$

where Nu is the Nusselt number of the fluid, k_w is the saturated liquid thermal conductivity, and D is the diameter of the channel. Substituting Eq. (21) into (20) yields

$$\dot{Q} = \frac{Nuk_wA_p}{D}(T_w - T), \quad (22)$$

Nu is obtained from a two-phase flow semi-empirical correlation by Lin et al. (1979).

$$Nu = 190C_s\left(\frac{p}{p_c}\right)^{0.25}\left(\frac{qD_e}{\Delta h_v\mu_l}\right)^{0.7}e^{-0.125x}. \quad (23)$$

Eq. (23) employs dimensional analysis to correlate heat transfer data and was been derived from two of the more generally accepted and proven correlations by Rohsenow (1952) and Borishanskii (1973), where C_s is the surface condition of the wall, p is the working pressure of the fluid, p_c is the critical pressure of the fluid, q is the heat heater input flux density, D_e is the effective diameter of the channel, h_v is the latent heat of vaporization, μ_l is the saturated liquid viscosity, and x is the average vapor quality. Based on experimental work by Lin et al. (1979), mass flow rate does not influence heat transfer coefficient but vapor quality has a slight influence. At any instant, average flux density, mass flow rate, and entrance enthalpy, the time average heat transfer coefficient along the tube decreases by a small amount with and increase of time average vapor quality, x. At the regimes with higher average vapor quality, mist flow occupies more time and as a result, since mist flow is lower than that of other regimes, the time average heat transfer coefficient h at such sections become lower.

For the quality range 0–1, the exponential function $e^{-0.125x}$ varies almost linearly with respect to the average quality x. The exponential function $e^{-0.125x}$ versus the average quality range 0–0.5 is equivalent to a linear function or

$$f(x) = e^{-0.125} \approx -0.12x + 1.0. \quad (24)$$

Substituting Eq. (24) into (23) yields

$$Nu = 190C_s\left(\frac{p}{p_c}\right)^{0.25}\left(\frac{qD_e}{\Delta h_v\mu_l}\right)^{0.7}(-0.12x + 1.0) \quad (25)$$

or

$$Nu = Nu_1 - 0.12Nu_1x, \quad (26)$$

where

$$Nu_1 = 190C_s\left(\frac{p}{p_c}\right)^{0.25}\left(\frac{qD_e}{\Delta h_v\mu_l}\right)^{0.7}. \quad (27)$$

Substituting Eq. (25) into (22) yields

$$\dot{Q} = \frac{190C_sk_wA_p}{D}\left(\frac{p}{p_c}\right)^{0.25}\left(\frac{qD_e}{\Delta h_v\mu_l}\right)^{0.7} \times (T_w - T)(-0.12x + 1.0) \quad (28)$$

or

$$\dot{Q} = Nu_2 - Nu_3x, \quad (29)$$

where

$$Nu_2 = \frac{Nu_1k_wA_p}{D}(T_w - T) \quad (30)$$

and

$$Nu_3 = \frac{0.12Nu_1k_wA_p}{D}(T_w - T). \quad (31)$$

Power input into the fluid $\dot{Q}$ is also a function of mass flow rate W and quality or

$$\dot{Q} = 2xh_{fg}W - Wh_{so} + Wh_f. \quad (32)$$

Therefore, substituting Eq. (29) into (27), the average quality x can be expressed as the function of the mass flow rate only or

$$x = \frac{Nu_2 + W(h_{so} - h_f)}{(2h_{fg}W - Nu_3)}. \quad (33)$$

Substituting Eq. (33) into (27) yields

$$\dot{Q} = Nu_2 - Nu_3\frac{Nu_2 + W(h_{so} - h_f)}{(2h_{fg}W - Nu_3)}. \quad (34)$$

Substituting Eq. (34) into (19) yields

$$\frac{dT_w}{dt} = \frac{1}{m_Hc_H}\left(\dot{Q}_H - Nu_2 + Nu_3\frac{Nu_2 + W(h_{so} - h_f)}{(2h_{fg}W - Nu_3)}\right). \quad (35)$$

3. Results and discussion

In Fig. 2 we reproduce the surge tank outlet pressure trace for pressure drop oscillations from Yüncü's work for W_{si} = 0.006 kg/s for a channel similar to that in Fig. 1 with a heat input $\dot{Q}_H$ of 425 W (Yüncü, 1990). We consider $L \approx 1.0$ m,

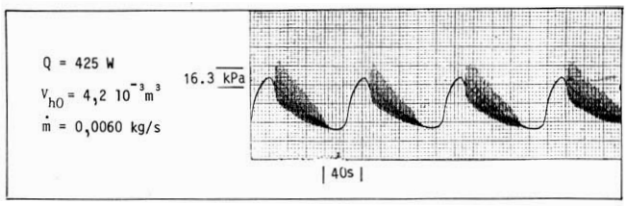

Fig. 2. A trace of heater inlet pressure versus time oscillations for 0.006 kg/s from Yüncü (1990).

$D = 5 \times 10^{-3}$ m, $H_{st} = 0.275$ m, $H_{si} = 0.137$ m, $A_s = 0.03048$ m^2, $A = 1.963 \times 10^{-5}$ m^2, and $p_a = 2 \times 10^5$ Pa absolute, $\rho_H = 8400$ kg/m^3, $\rho_f = 1483$ kg/ m^3, $m_H = \rho_H L A_s$, and, $c_H = 420$ kJ/kg K. These dimensions are comparable to those of Yüncü (1990).

The numerical solution to Eq. (18) for $W_{si} = 0.006$ kg/s and for $W_{sin} = 0.0054$ kg/s with a heat input of 425 W is based on Fig. 3, the numerical solution of the heater inlet pressure versus time trend has the same period and amplitude as the heater inlet pressure versus time trend (see Fig. 2) obtained from experimental results by Yüncü. The trace of the mass flow rate versus time for the heat input of 425 W is shown in Fig. 4.

The trace of the change in the liquid height inside the surge tank for the heat input of 425 W is shown in Fig. 5.

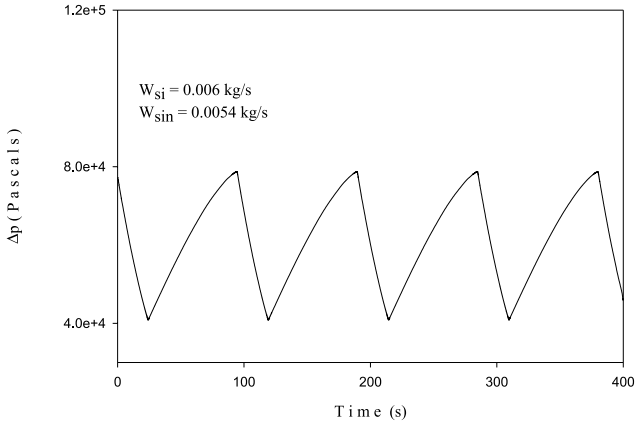

Fig. 3. A trace of heater inlet pressure versus time.

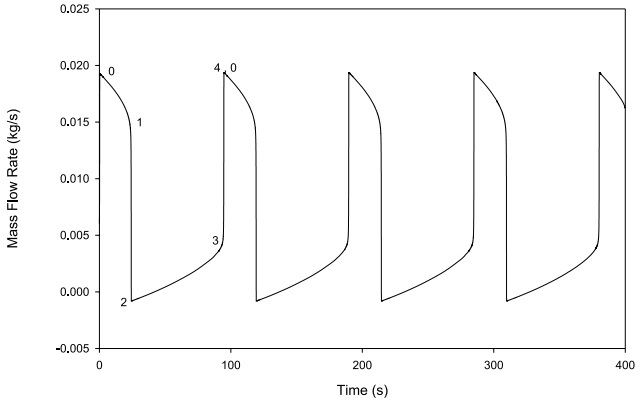

Fig. 4. A trace of heater mass flow rate versus time.

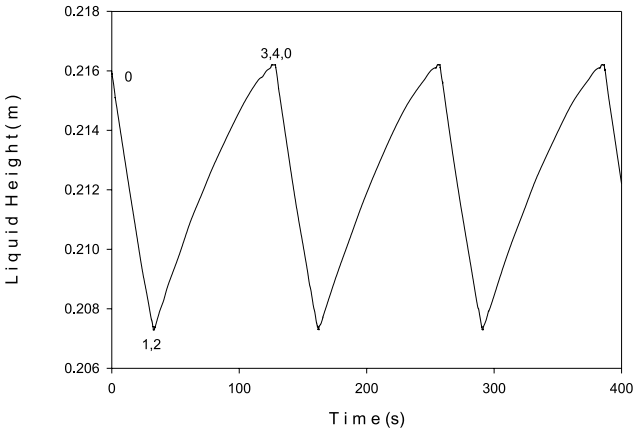

Fig. 5. A trace of the change in liquid height versus time.

The change in the heater wall temperature along the heated channel for the heat input of 425 W is shown in Fig. 6.

The phase portrait of the pressure difference between the surge tank surface and the channel outlet versus mass flow rate curve for 425 W is generated and imposed on the steady-state pressure drop versus mass flow rate curve in Fig. 7 for a reduction in the surge tank inlet mass flow rate for W_{si} to W_{sin}.

Using Fig. 7, the limit cycle observed in Figs 3–6 can be explained as follows, Let us say we are operating at point 0 shown in Fig. 7 and we very quickly (or instantaneously) reduce the surge tank inlet mass flow rate from W_{si} to a new, steady mass flow rate $W_{sin} = 0.9W_{si}$, which is less than the mass flow rate corresponding to point 1, in Fig. 7. Since the new and steady surge tank inlet mass flow rate is less than the surge tank outlet mass flow rate during a short time period after the surge tank inlet mass flow rate has been reduced, applying conservation of mass to the surge tank shows the liquid level in the surge tank drops. Assuming that the gas temperature is constant at the liquid temperature in the surge tank, the ideal gas law indicates that the gas pressure drops due to the gas expansion. Since the gas pressure is a significant driving force for the surge tank outlet mass flow rate through the outlet channel, the falling gas pressure reduces this outlet mass flow rate from that at point 0 toward the outlet mass flow rate at point 1. The gas pressure (and hence pressure difference be-

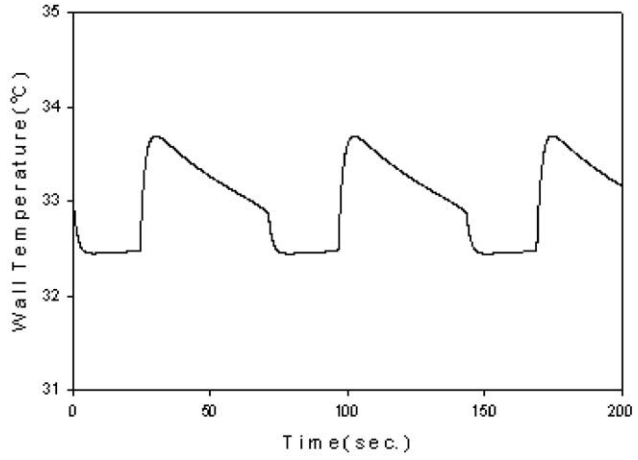

Fig. 6. Time history of the thermal wall temperature for the input of 425.

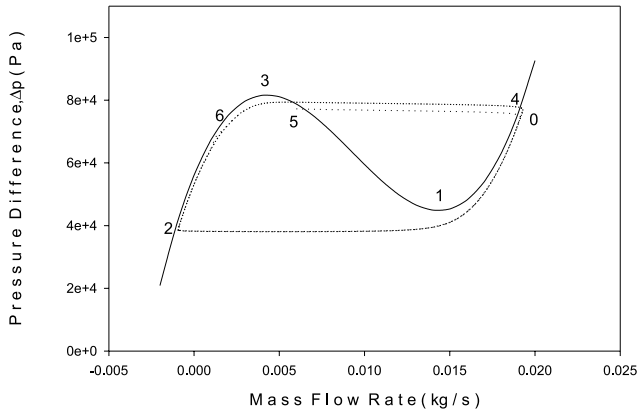

Fig. 7. A phase portrait of the pressure difference versus mass flow rate imposed on the steady-state curve.

tween the channel inlet and the channel outlet) and the outlet mass flow rate decrease along (or close to) the steady state pressure difference – mass flow rate characteristic for the heated channel. As this pressure difference drops just below the pressure difference for point 1, the outlet mass flow rate W jumps immediately to the outlet mass flow rate at point 2, as it is the only outlet mass flow rate compatible to this lower pressure difference. The surge tank outlet mass flow rate at point 2 is now less than the surge tank steady inlet mass flow rate W_{sin} and the surge tank liquid level rises. This compresses the gas in the surge tank and increases the pressure difference between the channel inlet and the channel outlet which causes the outlet mass flow rate to increase along (or close to) the steady state pressure difference – mass flow rate characteristic toward the outlet mass flow rate at point 3. The surge tank outlet mass flow rate at point 3 is still less than the surge tank steady inlet mass flow rate W_{sin}, so the surge tank liquid level still increases, the gas pressure (and pressure difference between the channel inlet and the channel outlet) still increases to a value above that of point 3, and the outlet mass flow rate jumps immediately to the outlet mass flow rate at point 4, as this is the only outlet mass flow rate compatible to this higher pressure difference. The surge tank outlet mass flow rate at point 4 is now greater than the surge tank steady inlet mass flow rate W_{sin}, the surge tank liquid level drops, and the gas pressure (or pressure difference) decreases along (or close to) the steady-state pressure difference – mass flow rate characteristic toward point 1, and the cycle continues.

Continuing the above hypothesis, let us say we are again operating at point 0 shown in Fig. 7 and we very quickly reduce the inlet flow rate W_{si} to a new, steady mass flow rate W_{sin} which, this time, is greater than that of the mass flow rate corresponding to point 1 in Fig. 7. The new and steady surge tank inlet mass flow rate is again less than the surge tank outlet mass flow rate during a short time period after the surge tank inlet mass flow rate has been reduced. Again applying conservation of mass to the surge tank shows the liquid level in the surge tank drops and the ideal gas law shows that the gas pressure drops due to the gas expansion. This time the gas pressure and hence the pressure difference between the channel and the channel outlet does not drop below that corresponding to point 1 and the outlet mass flow rate stabilizes at an outlet mass flow rate equal to the new, steady inlet mass flow rate greater than that at point 1. This stabilization can occur either in an underdamped manner or in an overdamped manner. An underdamped oscillation would most likely occur when there is light damping in the heated channel (possibly a larger diameter channel) and an overdamped response would most likely occur when there is heavy damping in the heated channel (possibly a very small diameter channel or some damping mechanism like an orifice). This behavior on the right most positive slope portion of the characteristic is similar to unheated channels or single-phase systems. The present model is uses 5 mm inner diameter as suggested in Yüncü (1990). In the model by Padki et al. (1992), 7.5 mm is used. The present model should work for inner diameters ranging from 2 to 8 mm.

Consider that we are operating at point 0 and a small decrease in flow rate occurs. At this flow rate just to the left of point 0, the available pressure difference is greater than the required pressure difference between the gas and the channel exit and the flow rate is forced to increase to that at point 0. Next, consider that we are operating at point 0 and a small increase in flow rate occurs. At this flow rate just to the right of point 0, the available pressure difference is less than the required pressure difference between the gas and the channel exit and the flow rate is forced to decrease to that at point 0. Therefore, point 0 with the available pressure difference curves makes point 0 a stable condition.

Next, consider that we are at point 5 and a small decrease in flow rate occurs. At this flow rate just to the left of point 5, the available pressure difference is less than the required pressure difference between the gas and the channel exit and the flow rate is forced to decrease to that at point 6. Next, consider that we are operating at point 5 and a small increase in flow rate occurs. At this flow rate just to the fight of point 5, the available pressure difference is higher than the required pressure difference between the gas and the channel exit and the flow rate is forced to increase to that at point 0. Therefore, point 5 with the available pressure difference curves makes point 5 an unstable condition.

4. Conclusions

A two-phase flow model with boiling and constant heat input has been developed for a surge tank with a constant inlet flow rate into the surge tank and an outlet flow rate through a horizontally heated channel. The required values of the steady-state pressure difference and mass flow rate are obtained from Yüncü's experimental data (Yüncü, 1990). The theoretical simplified two-phase model is verified against Yüncü's experimental model for validity. The relaxation oscillations observed for the two-phase flow model are analogous to the behavior of the van der Pol oscillator.

An overdamped flow rate was described as occurring on the positive slope portion of the steady-state pressure difference – mass flow rate characteristics curve. An underdamped oscillation would likely occur when there is light damping in the heated channel (possibly a larger diameter channel) and an overdamped response would likely occur when there is heavy damping in the heated channel (possibly a very small diameter channel or some damping mechanism like an orifice). Since boiling does not start to occur until the negative slope portion of the steady-state pressure difference – mass flow rate characteristic curve, this behavior on the right most positive slope portion of the characteristic is similar to unheated channels or single phase systems.

References

Borishanskii, V.M., 1973. A theoretical basis for the thermal calculation of a steam generator in sub-critical regime. Heat Transfer Soviet Research 5.

Gürgenci, H., Kakaç, S., Veziroğlu, T.N., 1976. Pressure-drop and density – wave instability threshold in boiling channels. In: Kakaç, S., Mayinger, F. (Eds.), Two-Phase Flows and Heat Transfer 1, Proceedings of NATO Advanced Study Institute, Istanbul, Turkey, August.

Gürgenci, H., Veziroğlu, T.N., Kakaç, S., 1983. Simplified nonlinear description of two-phase flow instabilities in vertical boiling channel. Int. J. Heat Mass Transfer 26 (5).

Kakaç, S., 1976. Boiling flow instabilities in multi-channel system. In: Kakaç, S., Mayinger, F. (Eds.), Two-Phase Flows and Heat Transfer, vol. 1. Proceedings of NATO Advanced Study Institute, Istanbul, Turkey, August.

Kakaç, S., Veziroğlu, T.N., 1982. A review of two-phase flow instabilities. In: Kakaç, S., Ishii, M. (Eds.), Advances in Two-Phase Flows and Heat Transfer 11, Proceedings of NATO Advanced Research Workshop, Spitzingsee, Germany, September.

Kakaç, S., Veziroğlu, T.N., Padki, M.M., Fu, L.Q., Chen, X.J., 1990. Investigation of thermal instabilities in a forced convection upward boiling system. Exp. Thermal Fluid Sci. 3.

Lin, S., Lee, P.M., Wang, R.L., 1979. Self induced oscillations in a electrical heating boiler. In: Veziroglu, T.N. (Ed.), Multiphase Transport: Fundamentals, Reactor Safety Applications, vol. 3. Proceedings of the Multi-Phase Transport and Heat Transfer, Miami, FL.

Maulbetsch, J.S., Griffith P., 1966. System-induced instabilities in forced convection flows with subcooled boiling. In: Proceedings of the Third International Heat Transfer Conference, AlChE, vol. 4, pp. 247–257.

Padki, M.M., Liu, H.T., Kakaç, S., 1991. Two-phase flow pressure type and thermal oscillations. Int. J. Heat Fluid Flow 2 (3).

Padki, M.M., Palmer, K., Kakaç, S., Veziroğlu, T.N., 1992. Bifurcation analysis of pressure drop oscillations and the Ledinegg instability. Int. J. Heat Mass Transfer 35 (2).

Rohsenow, W.M., 1952. A method of correlating heat transfer data for surface boiling of liquids. Trans. ASME 74.

Stenning, A.H., Veziroğlu, T.N., Callahan, G.M., 1967. Pressure-drop oscillations in forced convection flow with boiling. In: Symposium on Two-Phase Flow Dynamics, Eindhoven.

Strogatz, S.H., 1995. Nonlinear Dynamics and Chaos. Addison-Wesley, Reading, MA.

Van der Pol, B., 1927. Forced oscillations in a circuit with non-linear resistance. Philos. Mag. 3 (7).

Yüncü, H., 1990. An experimental and theoretical study of density wave and pressure drop oscillations. Heat Transfer Eng. 11.

Yüncü, H., Yildirim, O.T., Kakaç, S., 1990. Two-phase flow instabilities in a horizontal single boiling channel. Appl. Scientific Res. 48.